Genetic consequences of Quaternary climatic oscillations in the Himalayas: *Primula tibetica* as a case study based on restriction site-associated DNA sequencing

Guangpeng Ren[1,2,3], Rubén G. Mateo[1,4], Jianquan Liu[3], Tomasz Suchan[1], Nadir Alvarez[1], Antoine Guisan[1,4], Elena Conti[5] and Nicolas Salamin[1,2]

[1]Department of Ecology and Evolution, Biophore, University of Lausanne, 1015 Lausanne, Switzerland; [2]Swiss Institute of Bioinformatics, Quartier Sorge, 1015 Lausanne, Switzerland; [3]State Key Laboratory of Grassland Agro-Ecosystem, School of Life Science, Lanzhou University, Lanzhou, 730000 Gansu, China; [4]Institute of Earth Surface Dynamics, Geopolis, University of Lausanne, 1015 Lausanne, Switzerland; [5]Department of Systematic and Evolutionary Botany and Botanic Garden, University of Zurich, Zollikerstrasse 107, 8008 Zurich, Switzerland

Summary

• The effects of Quaternary climatic oscillations on the demography of organisms vary across regions and continents. In taxa distributed in Europe and North America, several paradigms regarding the distribution of refugia have been identified. By contrast, less is known about the processes that shaped the species' spatial genetic structure in areas such as the Himalayas, which is considered a biodiversity hotspot. Here, we investigated the phylogeographic structure and population dynamics of *Primula tibetica* by combining genomic phylogeography and species distribution models (SDMs).

• Genomic data were obtained for 293 samples of *P. tibetica* using restriction site-associated DNA sequencing (RADseq). Ensemble SDMs were carried out to predict potential present and past distribution ranges.

• Four distinct lineages were identified. Approximate Bayesian computation analyses showed that each of them have experienced both expansions and bottlenecks since their divergence, which occurred during or across the Quaternary glacial cycles. The two lineages at both edges of the distribution were found to be more vulnerable and responded in different ways to past climatic changes.

• These results illustrate how past climatic changes affected the demographic history of Himalayan organisms. Our findings highlight the significance of combining genomic approaches with environmental data when evaluating the effects of past climatic changes.

Introduction

Biodiversity hotspots that harbor extremely high species richness are often associated with mountains (Myers *et al.*, 2000). The origin and evolution of biodiversity in mountainous areas are highly dependent on historical orogenesis and associated climatic changes (Hoorn *et al.*, 2010; Favre *et al.*, 2014; Liu *et al.*, 2014; Wen *et al.*, 2014). The alteration of topography and past climatic changes associated with mountain uplifts can cause fragmentation of species distributions, which can lead to reduced gene flow between isolated populations. This process initiates allopatric divergence that can ultimately drive populations towards speciation (Mayr, 1963; Rice & Hostert, 1993). It has recently been proposed that mountain uplift can also result in divergence and speciation in the face of gene flow across a continuous altitudinal gradient (Filatov *et al.*, 2016). In this context, climatic oscillations during the Quaternary could have reinforced allopatric divergence and driven intraspecific divergence as well as local

adaptation (Davis & Shaw, 2001; Hewitt, 2004; Li *et al.*, 2013; Liu *et al.*, 2013; Schorr *et al.*, 2013), as populations experienced repeated cycles of retreat to refugia and postglacial expansions (Abbott *et al.*, 2000; Avise, 2000; Petit *et al.*, 2003). The demographic changes involved in these range shifts affected the spatial patterns of genetic variation within and among populations (Hewitt, 2004). However, the detailed processes involved are still poorly understood in most species.

The Himalayas, especially their core region (i.e. the Qinghai-Tibet Plateau, QTP), comprise one of the key high-altitude biodiversity hotspots in the world (Myers *et al.*, 2000). The uplift of the QTP created a large altitudinal gradient across the region spanning from 500 to 8848 m (Wu, 1987). The eastern Himalayas are associated with deep valleys and characterized mainly by a warm and wet climate (Liu *et al.*, 2013; Fig. 1). By contrast, the central and western Himalayas are characterized by a cold and dry climate because of high mountains forming the southern ridge of the Himalayas (six mountain summits exceed
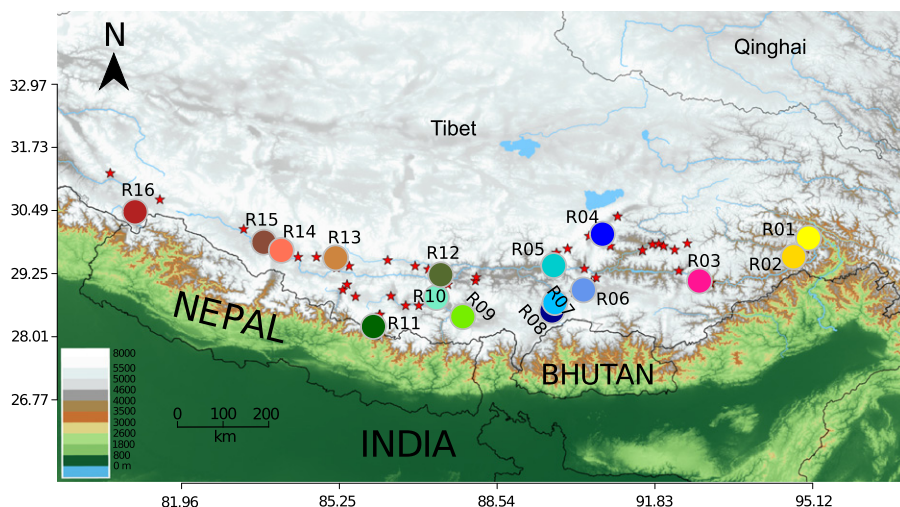
Fig. 1 Sampling locations of all 61 populations of *Primula tibetica* (red stars) and the 16 selected populations (large colored circles) used for genomic analyses in this study.

8000 m; Favre *et al.*, 2014) and the high average altitude (> 4000 m). The geological events created large and profound ecological heterogeneity (Li *et al.*, 1995; Shi *et al.*, 1998; Yin & Harrison, 2000), which potentially led to divergent selection and adaptation associated with different ecological niches that created numerous endemic species (Wu, 1987; Favre *et al.*, 2014; Liu *et al.*, 2014). It is also proposed that these geological events have provided opportunities for species to migrate out of the region (Liu *et al.*, 2006; Jia *et al.*, 2012; Zhou *et al.*, 2013; Wen *et al.*, 2014; Ren *et al.*, 2015). Although the region is assumed to be particularly vulnerable to climatic changes (Zheng, 1996; Yao *et al.*, 2007), the pattern and extent of glaciation during the Quaternary and their effects on the evolutionary history of species within the Himalayas have not yet been fully examined, especially based on population genomic data.

By contrast, large-scale phylogeographic studies based mainly on a few plastid DNA regions have been conducted on species occurring in the QTP (e.g. Zhang *et al.*, 2005; Meng *et al.*, 2007; Yang *et al.*, 2008; Wang *et al.*, 2009; Shimono *et al.*, 2010; Qiu *et al.*, 2011; Li *et al.*, 2013; Liu *et al.*, 2013). The existence of a deep divergence between the Himalayan populations and those occurring in other regions of the plateau was already inferred, and extensive private haplotypes have been found in the Himalayan populations (e.g. Opgenoorth *et al.*, 2010; Wang *et al.*, 2010b; Jia *et al.*, 2011), implying that multiple plant refugia probably existed in the Himalayas. However, these studies were unable to detect the detailed effects of past climatic changes on the demographic history of the studied organisms. Next-generation sequencing (NGS) methods (Davey *et al.*, 2011), such as restriction site-associated DNA sequencing (RADseq; Peterson *et al.*, 2012), which have been shown to be highly effective in tracing postglacial recolonization and reconstructing detailed demographic histories of species (e.g. Emerson *et al.*, 2010; Lanier *et al.*, 2015), could provide opportunities to better understand the effects of past climatic changes in driving speciation and evolution of alpine organisms in the Himalayas.

In this study, we focus on *Primula tibetica* (Primulaceae), one of the most widely distributed alpine plant species in the Himalayas (Hu & Kelso, 1996; Richards, 2003). *P. tibetica* is an insect-pollinated (mostly by bees), heterostylous, herbaceous, perennial plant that occurs in diverse habitats at elevations ranging from 2600 to 5000 m (Hu & Kelso, 1996). Its scape is sometimes hidden among the leaves or can be as long as 13 cm. *P. tibetica* is an outcrossing small herb of variable height (2–13 cm) that disperses its seeds largely by gravity and usually grows in wet meadows or along hill streams (Hu & Kelso, 1996; Richards, 2003). Previous biogeographic analyses have indicated that *P. tibetica* originated in the Himalayas after the recent QTP uplift (i.e. 3.4–1.6 million yr ago (Ma); Ren *et al.*, 2015) and subsequent climatic oscillations during the Quaternary are likely to have played important roles in its intraspecific divergence and demographic history. This herbaceous species hence represents an ideal candidate to evaluate the effects of past climatic changes on a species' evolutionary history in the Himalayas. We use an integrative approach combining genomic phylogeography with niche modeling (e.g. Schorr *et al.*, 2012) to elucidate the divergence and demographic history of *P. tibetica*. The aims of our study are to identify the phylogeographic pattern of this species in the Himalayas and the factors that triggered its intraspecific divergence; to reconstruct a detailed demographic history of *P. tibetica*; and to combine species distribution models with approximate Bayesian computation (ABC) modeling to evaluate the effects of Quaternary climatic changes on its demographic history. This study represents the first RADseq analysis of a plant species occurring in the QTP and contributes to a better understanding of the role played by Quaternary climatic changes on the present-day distributions of organisms in mountain ranges.

Materials and Methods

Sampling, RAD library preparation and sequencing

We sampled a total of 61 populations (10–40 individuals for each population) of *Primula tibetica* Watt in Tibet using the distribution described in Flora of China (Hu & Kelso, 1996) as a reference to include all the relevant regions for the species. All materials were dried and stored in silica gel in the field. We selected 16 populations for the genetic study (Fig. 1; Supporting

Information Table S1) that were representative of both the geographical distribution and the diversity of ecological niches of *P. tibetica*. We estimated the latter by extracting the 19 bioclimatic variables of WorldClim (http://www.worldclim.org/current) from the occurrences of the individuals sampled in the 61 populations. We did a principal component analysis (PCA) using the PRCOMP function in the STATS package of R (R Core Team, 2012) and identified the 16 populations based on the PC1 and PC2 axes (which explained nearly 80% of the variance; Fig. S1). Fifteen to 20 individuals were chosen from each population, which gave us a total of 293 individuals that were processed with RADseq. The leaf tissues were ground to dust using an electric tissue homogenizer. Total genomic DNA was then isolated using the DNeasy Plant Mini Kit (Qiagen) following the manufacturer's instructions. The extracted DNA was further cleaned with phenol-chloroform to remove salts or inhibitors that may reduce the activity of restriction enzymes.

The cleaned genomic DNA was individually barcoded and processed into three libraries using a double-digestion restriction fragment-based procedure following a modified protocol listed in the Supporting Information of Mastretta-Yanes *et al.* (2015). Briefly, the DNA was double-digested with *Eco*RI and *Mse*I restriction enzymes, followed by the ligation of Illumina adapter sequences and unique 8 bp barcodes that differed by at least three bases. Ligation products were purified with AMPure XP beads (Beckman Coulter, Brea, CA, USA) and amplified by Phusion High-Fidelity DNA Polymerase (New England Biolabs, Ipswich, MA, USA) with 12 cycles. The amplified products were pooled among samples and size-selected between 300 and 500 bp using AMPure XP beads with bead sample ratios of 0.8 and 0.2 modified from a protocol in https://www.neb.com/protocols/1/01/01/size-selection-e6270. The libraries were sequenced using single-end reads 100 bp in length in three lanes of Illumina HiSeq2500 according to the manufacturer's instructions.

Processing of Illumina data

Single-end Illumina reads were processed into RAD-tags using the STACKS-1.30 software pipeline (Catchen *et al.*, 2011, 2013) based on its ease of use, features and performance (Davey *et al.*, 2013). Initially, samples were demultiplexed with PROCESS_RADTAGS. Reads with an average Phred score of at least 30 and an unambiguous barcode and restriction cut site were retained. All reads were trimmed to 60 bp in length. The raw data were deposited in GenBank (accession no. PRJNA339808). Next, the USTACKS program was used for the *de novo* assembly of raw reads into RAD-tags. We used all 293 samples to build a catalog in CSTACKS and matched each sample against the catalog to identify alleles in SSTACKS. The execution of these components was accomplished using the DENOVO_MAP.PL script with the following settings: minimum number of reads to create a stack, $m = 3$; maximum distance allowed between stacks, $M = 2$; maximum number of mismatches allowed between loci. $n = 2$; *-t* flag to remove or break up highly repetitive RAD-tags during the USTACKS component and upper bound of error rate, $\varepsilon = 0.1$. A conservative bound was preferred over the unbounded model

because the latter has been shown to underestimate heterozygotes (Catchen *et al.*, 2013). We used RXSTACKS to further filter the data to increase quality, correct single nucleotide polymorphism (SNP) calls and remove haplotypes that were in excess. The RXSTACKS used the output from the DENOVO_MAP.PL script as input combined with the following filters: *−conf_filter −conf_lim 0.25 −prune_haplo −model_type bounded −bound_high 0.1 − lnl_lim -10.0 −lnl_dist*. After RXSTACKS, CSTACKS and SSTACKS were run again with the same setting as before to rebuild the catalogue of reads. To test the sensitivity of our results to different sets of parameters, we further processed our RAD data with two other parameter settings: using the same settings as earlier except for $M = 3$ and $n = 3$, and trim the reads to 90 bp in length ($M = 3$, $n = 3$ and 90 bp); and $M = 5$, $n = 3$ and 90 bp. The results of the population structure analyses based on the three datasets were
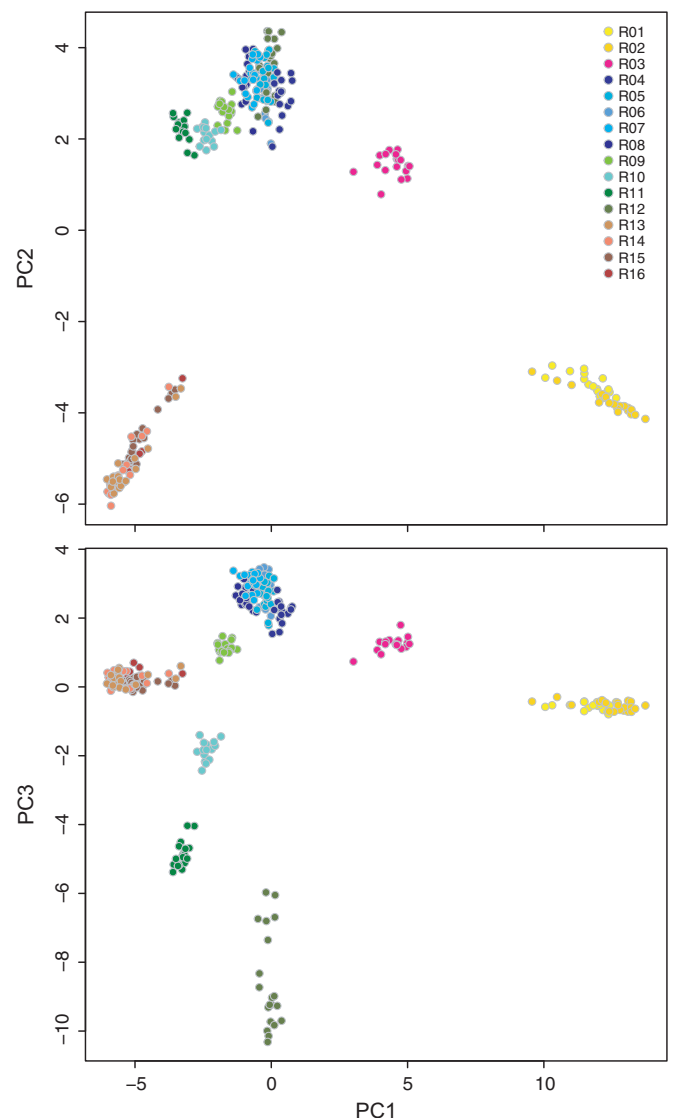

Fig. 2 Distribution of individuals of *Primula tibetica* along principal component (PC) scores (PC1, 20% vs PC2, 9.4%; PC1 vs PC3, 6.6%) of genetic variation based on the analysis of single nucleotide polymorphism (SNP) dataset; individuals are color-coded according to their population identities (see Fig. 1).

qualitatively similar (Figs 2, S2), and we only presented results from our analyses based on the dataset generated by $M = 2$, $n = 2$, given the increased number of assembled loci (3509 vs 2822 vs 2031).

We filtered the catalog of reads using the POPULATIONS module to produce datasets for downstream population genetic analyses. We first retained RAD-tags with a minimum stacks depth, $m = 3$. Polymorphic RAD loci that were present in at least 50% of the individuals of each population and in all 16 populations were retained. Potential homeologs were excluded by removing loci showing heterozygosity > 0.5 within samples (Hohenlohe *et al.*, 2011). We further filtered our dataset with a minor allele frequency (MAF) > 0.01 and kept only biallelic SNPs to comply with the assumptions of the current methods for analyzing SNP data. Population genetic statistics, including nucleotide diversity (π), Wright's F-statistic (F_{IS}) and observed heterozygosity (H_{obs}) were calculated using the POPULATIONS program in the STACKS pipeline (Holsinger & Weir, 2009; Catchen *et al.*, 2013). Pairwise F_{ST} values were calculated among populations in GENODIVE v.2.0b27 (Meirmans & Van Tienderen, 2004), and significance was determined using 1×10^4 permutations.

Characterization of population genetic structure

We first identified population genetic structure using the Bayesian method implemented in STRUCTURE 2.3.4 (Pritchard *et al.*, 2000). SNPs located at the same locus are physically linked and cannot be handled by STRUCTURE. We thus filtered out linked SNPs using the *–write_single_snp* option in the POPULATIONS script. Analyses were performed under the 'Admixture model' and the 'Correlated allele frequency model' with K-values ranging from 1 to 18. Ten independent runs were performed for each value of K using 1×10^5 generations for the burnin and 2×10^5 generations for the sampling. The optimal K was chosen using the delta-K method of Evanno *et al.* (2005) as implemented in STRUCTURE HARVESTER (Earl & vonHoldt, 2012). The coefficient for cluster membership of each individual was averaged across the 10 independent runs using CLUMPP (Jakobsson & Rosenberg, 2007) and plotted using DISTRUCT (Rosenberg, 2004). We further performed a PCA to visualize the major axes of variation of the population genetics using the *adegenet* package (*glPCA* function; Jombart, 2008) in R. Finally, we estimated a maximum-likelihood phylogeny of the 16 populations from unlinked SNPs with a GTR + G model using PHYML 3.0 (Guindon *et al.*, 2010). *Primula nutans* and *Primula fasciculata* were used as outgroups. Nodal support was estimated using 1000 bootstrap replicates.

Relationships between genetic differentiation and geography

The first two components of the PCA performed on the genetic data and the geographic coordinates (latitude and longitude) of the 16 populations were used in a Procrustes analysis using the R package VEGAN (Oksanen *et al.*, 2013). This analysis minimizes the sum of squared Euclidean distances between two sets of points by rotating one set of points to match the other, while preserving the relative distances among all points within the map (Wang *et al.*, 2012). The similarity of the two maps is quantified using the Procrustes similarity statistic $t_0 = \sqrt{1 - D}$, where D is the minimum sum of the squared Euclidean distances between the two maps, scaled to range between 0 and 1 (Wang *et al.*, 2010a, 2012). We used the PROTEST function in VEGAN to test, using 1×10^5 permutations, the probability of observing a similarity statistic higher than the observed t_0 if no geographic pattern is assumed (Wang *et al.*, 2012). We also tested for the presence of isolation by distance (IBD) by comparing pairwise F_{ST} values and Euclidean geographic distances among populations within and among groups that were identified by the PCA and STRUCTURE analyses. We further tested the significance of the relationship between geographic and genetic distance within groups with a Mantel test in the package VEGAN using 1×10^5 permutations.

Estimates of historical demography

To decipher the historical demography of *P. tibetica*, we estimated divergence times, admixture and changes in population size among different population groups using ABC. We pooled the population samples into four 'groups' (eastern group E, R01–R02; central-eastern group CE, R03; central group C, R04–R12; western group W, R13–R16) for the ABC simulations based on the first two axes of the PCA that captured the main characteristics in population histories (Fig. 2). We tested three competing scenarios using DIY-ABC v.2.1.0 (Cornuet *et al.*, 2010, 2014) based on the results from STRUCTURE and the phylogenetic tree (Fig. S3). In all scenarios, groups E and C diverged first and group W originated from group C. The scenarios modeled the possible hypotheses about the origin of the group CE, which can arise from either groups E or C, or be the result of an admixture between the two groups (Fig. S4a). We selected for these analyses a single SNP per locus, and the SNPs further had to be present in at least 70% of the individuals from each group and in all four groups. The simulated SNP dataset was generated following the algorithm proposed by Hudson (2002). We further chose MAF = 0.01 to increase the mean amount of genetic variation of both the observed and simulated datasets and to reduce the proportion of loci that may correspond to sequencing errors. We gave each scenario a uniform prior probability (Table S2) and selected all summary statistics to generate a reference table containing 3×10^6 simulated datasets (on average 10^6 per scenario). We used 1% of the simulated datasets closest to the observed data to estimate the relative posterior probabilities for each scenario via logistic and posterior distribution of historical demographic parameters according to the most likely scenario (Cornuet *et al.*, 2010). The time parameters are estimated in generations and converted into years by multiplying generation time, which was set to 1 yr for *P. tibetica*. Although there is no information of generation time for *P. tibetica*, filed observations are coherent with this assumption and other studies on related species of *Primula* have also used a generation time of 1 yr to study demographic history of *P. obconica* (Yan *et al.*, 2012). In addition, we also

considered the substructure (R11–R12) identified by the PCA and STRUCTURE as a fifth group for ABC modeling (Fig. S5). However, simulations based on five groups were not stable enough to provide a convincing outcome compared with the ABC modeling with four groups, which could further indicate that these two populations do not form a homogeneous cluster (see Notes S1 for a full description of the ABC modeling with five groups).

Finally, DIY-ABC was used to investigate changes in population sizes of the four groups in the recent past. We first selected only one SNP per locus and used two thresholds (i.e. SNP had to be present in at least 70% vs 80% of the individuals in each group) to generate datasets for each group. We then did PCA based on these datasets, and the two thresholds resulted in similar structure patterns for each group (Fig. S6). We used the datasets generated based on the 80% threshold for these ABC analyses, because they have fewer missing data and it saved computational time. We tested the following scenarios of demographic changes: continuous expansion since divergence; recent expansion; expansion followed by shrinkage; and expansion followed by shrinkage and a new expansion event (Fig. S7a; Wang *et al.*, 2016). We used the same strategy as earlier to choose the most likely scenario and estimate the parameters of interest.

Species distribution models

An ensemble of species distribution models (SDMs; Guisan & Zimmermann, 2000) was generated for *P. tibetica* using three different techniques: generalized linear model, gradient boosting machine and random forests, as implemented in the R package *biomod2* (Thuiller *et al.*, 2009; see Methods S1 for similar results with MAXENT as a fourth technique, and explanations therein; Fig. S8). A total of 58 species occurrences obtained directly from the filed collections were used as presence data to calibrate the models. We used the 19 bioclimatic variables of Worldclim (http://www.worldclim.org; Hijmans *et al.*, 2005) as environmental predictors. To avoid multicollinearity, we ran a Pearson correlation analysis to eliminate one of the variables in each pair with a correlation value higher than 0.8 (Dormann *et al.*, 2013). A set of seven variables was finally used to carry out the SDM (Methods S1). For a proper evaluation, models were calibrated on 70% of the data and evaluated on the remaining 30% using area under the curve (AUC) and true skill statistic (TSS) statistics (Allouche *et al.*, 2006). This sampling procedure was replicated 10 times. The potential distribution was considered as a consensus across statistical techniques (Mateo *et al.*, 2012) and their contribution to the ensemble was proportional to their AUC values. The consensus model was converted to a binary model (presence/absence) applying three different threshold criteria (Methods S1): thresholds that allow a maximum of 5% or 10% of omission error (i.e. omission error is the percentage of the real presence predicted as absences in the model; Fielding & Bell, 1997), and the threshold maximizing the AUC statistic. The consensus model was then projected onto different past climatic periods using the data available in the Worldclim dataset: the last interglacial (LIG; 0.12–0.14 Ma), the Last Glacial Maximum

(LGM; 0.022 Ma), and the mid-Holocene (MH; 0.006 Ma). For the MH and LGM we employed three different general circulation models (GCMs; Earth-system climatic models coupling the ocean, the atmosphere and the land surface; CCSM4, MIROC-ESM, MPI-ESM-P available from http://cmip-pcmdi.llnl.gov/cmip5/processed on www.worldclim.org). Only one GCM is available for the LIG period.

Results

Sequence data quality and processing

We sequenced 293 individuals of *P. tibetica* using three lanes of Illumina that produced a total of > 730 million reads. Over 560 million reads passed our quality controls and over 460 million reads were used in the assembly of the RAD-tags (Table S3). We obtained 3509 RAD loci containing 8930 SNPs that could be used for population genetics analyses. The dataset was used to estimate historical scenarios of *P. tibetica* containing 4882 single-SNP loci. Finally, four datasets containing 8579, 5401, 7777, and 10 431 single-SNP loci were used to estimate the changes in population sizes of groups E, C, CE and W, respectively.

Population structure

The first two axes of PCA identified four genetic groups and explained 20% and 9.4% of the total variation, respectively (Fig. 2). The first axis, PC1, showed considerable correspondence between the genetic data and the east–west geographic axis. The two eastern populations (R01, R02) and four western populations (R13–R16) formed two separate groups (groups E and W) that were located on the two extreme sides of the distribution. One central-eastern population (R03) and the rest of populations (R04–R12) were further isolated from the groups E and W by the second axis of the PCA (PC2; Fig. 2) and formed two other groups (groups CE and C), respectively. The third axis of the PCA (PC3; 6.6% of the total variation) showed a substructure within group C, with four populations separating gradually from the rest of five populations following the increase of geographic distance (Figs 1, 2). This pattern of population structure was also supported by the STRUCTURE analysis, which best explained the data with $K = 4$ (Fig. 3). Looking at intermediate K-values, the analyses showed that, at $K = 2$ (the second most probable number of genetic clusters; Fig. S9), group E first diverged from the rest of the populations (Fig. 3), which was also evident in the phylogenetic tree (Fig. S3). Group CE was always represented by admixed populations between the groups E and C at any values of K between 2 and 4 (Fig. 3). By contrast, the substructure (R09–R12) within group C identified by the PC3 was not always represented by admixed populations in STRUCTURE from $K = 2$ to $K = 4$. Moreover, the populations comprising this substructure were not clustered together along the PC3. We therefore did not include this substructure when performing ABC modeling (see more details in Notes S1 for the reason not including the substructure in ABC analyses). Finally, the Procrustes analysis identified a significant similarity score between the populations in
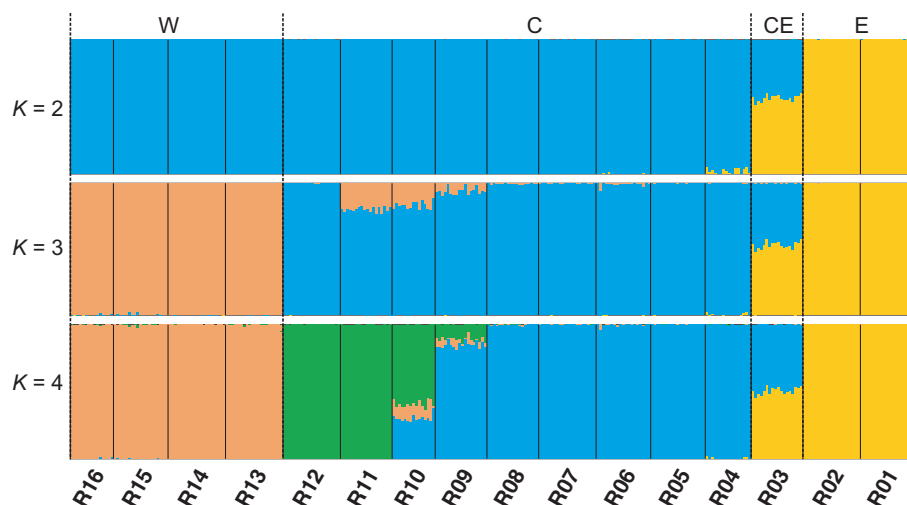
Fig. 3 Plots of posterior probabilities for individuals of *Primula tibetica* assigned to *K* genetic clusters from STRUCTURE analyses for *K* = 2–4. Populations are delimited by black lines, with the corresponding population names listed along the bottom of the plot. The four groups are delimited by a dashed black line. E, eastern group; CE, central-eastern group; C, central group; W, western group.

genetic PC space and their actual geographic locations ($t_0 = 0.815$, $P < 10^{-5}$). A graphical examination of the rotated genetic coordinates (Fig. 4) showed that individuals of *P. tibetica* were more genetically similar within each group than would be expected given the geographic distance among populations.

Genetic diversity and IBD

The average within-population genetic diversity π ranged from 0.0011 to 0.0044, when considering all genetic positions, including those not polymorphic anywhere in the dataset (Table 1). Group E exhibited the lowest genetic diversity, which was three times lower than the diversity measured in groups CE and C, or two times lower than that of group W. The same pattern was also suggested by other standard measures of genetic diversity (e.g. observed heterozygosities; Table 1).

Differentiation among populations was significant, with F_{ST} values ranging from 0.032 to 0.807 (Table S4). Genetic distances between populations of different groups increased with geographical distances > 200 km, but populations among groups located

at smaller geographical distances displayed high genetic divergence (Fig. 5a). The genetic distance between populations of the same group was, however, always smaller than the distances among groups, which is congruent with the strong genetic structure observed in *P. tibetica* (see earlier). Furthermore, genetic distances increased with larger geographic distances among populations within groups (Fig. 5a), which was consistent with the significant pattern of IBD when performing a Mantel test among populations of group C ($r = 0.51$, $P = 0.016$; Fig. 5b). Although genetic distances among populations of group W were small (Table S4), we found a strong effect of IBD on population differentiation of this group ($r = 0.99$, $P = 0.042$; Fig. 5b).

Estimates of historical demography

Approximate Bayesian computation modeling of the demographic history of *P. tibetica* indicated that the scenario depicting an origin of group CE as a result of admixture between groups C and E provided the best fit to our RADseq data (Fig. S4b), with posterior probabilities significantly higher than the other
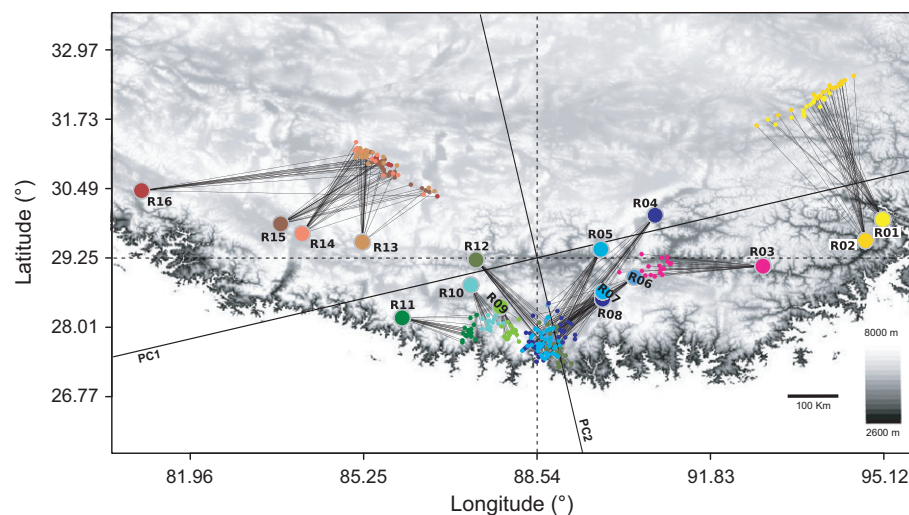

Fig. 4 Procrustes-transformed principal component analysis (PCA) plot of genetic variation with each individual of *Primula tibetica* mapped in PC space (the small circles) relative to the geographic location of populations (the larger circles). Black lines show the orientation of PC1 and PC2 for the genetic data (explaining 20% and 9.4% of the genetic variation, respectively) relative to the geographic longitude and latitudinal axes. The length of the line connecting individuals in PC space to their geographic location represents the extent of the deviation from the expected pattern of genetic variation based on geography.

Table 1 Population summary statistics calculated for the 3509 restriction site-associated DNA sequencing (RADSeq) loci

Genetic cluster	Population	n	Private (%)	Polymorphic (%)	π	H_{obs}	F_{IS}
Group E	R01	15	0.22	0.40	0.0013	0.0012	0.0003
	R02	18	0.19	0.34	0.0011	0.0011	0.0002
Group CE	R03	15	2.58	1.13	0.0037	0.0029	0.0021
Group C	R04	12	1.15	1.33	0.0038	0.0028	0.0029
	R05	15	1.31	1.50	0.0042	0.0033	0.0027
	R06	16	0.64	1.60	0.0041	0.0033	0.0025
	R07	17	10.64	1.82	0.0043	0.0035	0.0028
	R08	15	0.11	1.80	0.0044	0.0035	0.0029
	R09	15	0.36	1.40	0.0038	0.0031	0.0022
	R10	13	0.31	1.29	0.0038	0.0031	0.0019
	R11	16	0.48	0.67	0.0021	0.0018	0.0007
	R12	16	2.41	1.08	0.0031	0.0025	0.0019
Group W	R13	18	0.10	1.02	0.0029	0.0026	0.0009
	R14	18	0.01	1.09	0.0029	0.0026	0.0011
	R15	15	0.00	1.08	0.0030	0.0025	0.0014
	R16	13	0.10	0.84	0.0025	0.0024	0.0006

Included are the average number of individuals genotyped at each locus (n), the proportion of polymorphic single nucleotide polymorphisms (SNPs) unique to each population (% private), the percentage of SNPs (% polymorphic) in each population, the average nucleotide diversity (π), the average observed heterozygosity per locus (H_{obs}) and the Wright's inbreeding coefficient (F_{IS}). The total number of DNA sites (polymorphic + invariable) in the RADSeq loci is 210 540. E, eastern group; CE, central-eastern group; C, central group; W, western group.
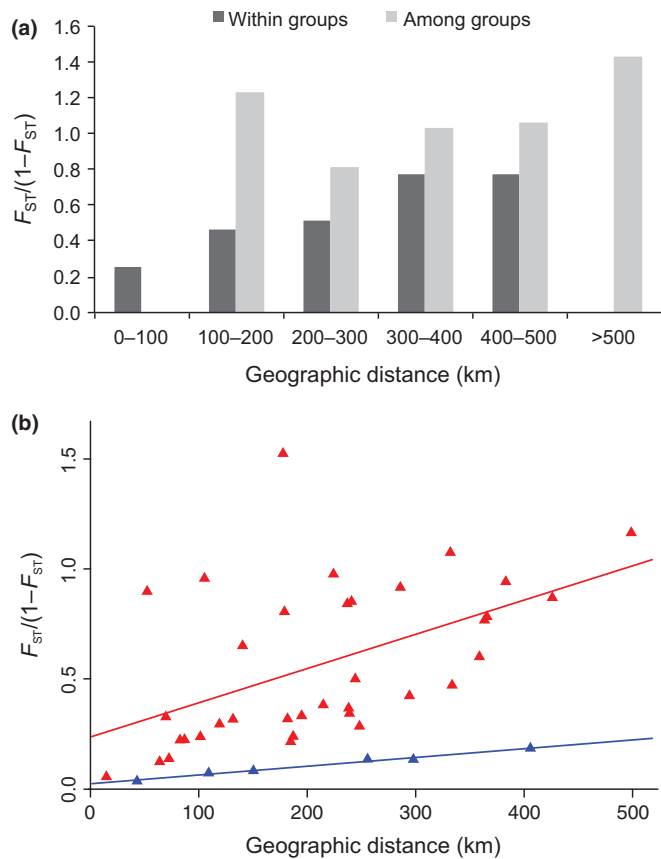

Fig. 5 (a) Averaged pairwise genetic differentiation between populations (F_{ST}) within and among genetic clusters for *Primula tibetica* based on six categories of geographic distances. (b) Correlations between pairwise genetic differentiation among populations (F_{ST}) within the central group (C; red; $r = 0.51$, $P = 0.016$) or the western (W) group (blue; $r = 0.99$, $P = 0.042$) and the geographic distance between populations.

scenarios (0.816, 95% credible interval: 0.797–0.834; Table S5). Modeling the changes in population size for each group recovered complicated demographic histories for the four groups of populations. Analyses for groups E and CE supported a scenario of 'expansion–shrinkage–expansion', while the two other groups were better modeled by a scenario of 'expansion–shrinkage' (Fig. S7; Table S5).

We estimated the divergence time and the population sizes as well as the timing and extent of these changes for the four groups. Group C was found to be the ancestral population of *P. tibetica* and started to expand its distribution *c.* 1.11 Ma (95% highest posterior density (HPD): 0.53–1.65 Ma; Table S6), followed by a slight bottleneck *c.* 0.063 Ma (HPD: 0.007–0.136 Ma). Group E diverged from the ancestral populations *c.* 0.76 Ma (HPD: 0.49–0.96 Ma; Table S7). It started to expand until *c.* 0.45 Ma (HPD: 0.15–0.92 Ma), before experiencing a severe bottleneck that decreased by *c.* 25 times its population size *c.* 0.12 Ma (HPD: 0.063–0.2 Ma). Then it quickly expanded just before LGM *c.* 0.037 Ma (HPD: 0.011–0.078 Ma) and reached the previous population size. During the first expansion of group E, it came into secondary contact with group C, exchanged genes and resulted in the formation of group CE *c.* 0.37 Ma (HPD: 0.213–0.525 Ma). Group CE experienced ancient expansion and shrinkage, and a recent expansion during the LGM (Fig. 6). Group W diverged from the ancestral population more recently, *c.* 0.095 Ma (HPD: 0.037–0.203 Ma), followed by expansion and a slight bottleneck during the LGM.

Species distribution models

The consensus models were highly accurate with regard to AUC (0.996) and TSS (0.998) values. Current potential distribution based on the three threshold approaches predicted similar results,
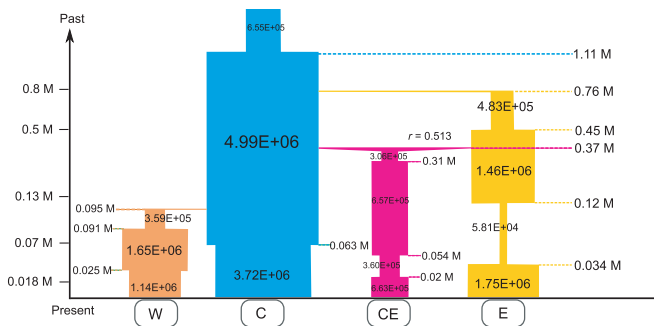
Fig. 6 Summary of inferred demographic history of the four genetic clusters of *Primula tibetica*. Changes in population sizes are integrated into the divergent scenario. Times on the vertical axis represent the glaciation periods that occurred in the Qinghai-Tibet Plateau (QTP) (Zheng *et al.*, 2002). Population sizes are indicated on each cylinder. Times of divergence and changes in population sizes are indicated by horizontal dashed lines. Only the mean values are shown (see Supporting Information Tables S6, S7 for 95% highest posterior density for all values). E, eastern group; CE, central-eastern group; C, central group; W, western group

Fig. 7 Habitat suitability of *Primula tibetica* predicted by species distribution models (SDMs) for present (a), mid-Holocene (MH) (b) and last Maximum Glacial (LGM) (c) using three techniques. SDMs for the MH and LGM are based on three climatic models. GCMs, general circulation models.

but the 5% omission error generally yielded a better representation of the actual distributions of the species, and we therefore presented all results based on the 5% omission threshold. The paleoclimatic conditions of LIG predicted large differences in annual mean precipitation in the Himalayas compared with the ones observed at the present, the MH or the LGM (Table S8). Therefore, it was not possible to predict the optimum climatic niche for the species during the LIG in this area considering the only available GCM model (Fig. S10; Methods S1). The predictions to MH conditions based on three GCMs (CCSM4, MIROC and MPI) yielded a continuous and less occupied overall distribution compared with current conditions, but larger distributions than the prediction at the LGM (Figs 7, S10). During the LGM, the three GCMs yielded similar patterns but fragmented palaeodistributions of *P. tibetica* (Figs 7, S10). All three GCMs suggested a main refugium in the central Himalayas and another in the southwestern Himalayas. The incongruence between models at the LGM yielded eastern or western expansions of suitable habitat compared with the predictions for the present and MH.

Discussion

Primula tibetica displays a strong geographic structure and we identified four main groups of populations that may represent multiple past refugia for this species in the Himalayas. IBD had an effect on genetic distance among populations within groups but not among groups. Instead, past climatic events were inferred to be the major factors in shaping the large-scale spatial genetic structure into four groups. The divergent times of the four groups based on ABC modeling are dated to < 1 Ma and the divergences are congruent with past glacial and interglacial events, providing support for intraspecific divergence driven by the Quaternary climatic oscillations. The use of genomic data coupled with extended evolutionary modeling allowed us to
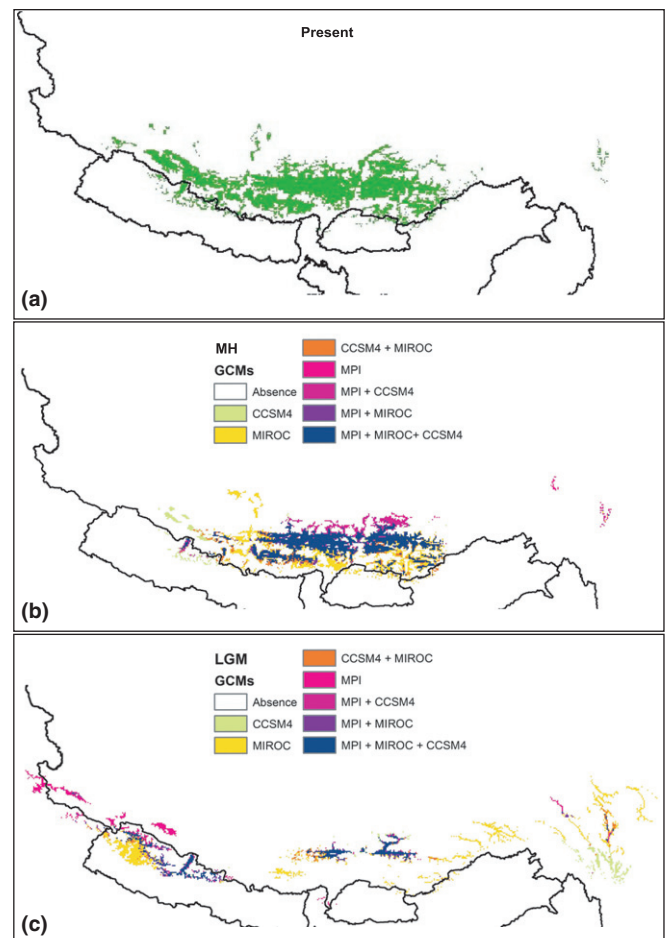
recover for the first time a detailed demographic history of a plant species native and endemic to the Himalayas. The changes in population sizes that we inferred, combined with species distribution modeling, suggest that the two easternmost and westernmost gene pools were more affected by past climatic changes than the ancestral populations. The response to climatic changes of populations of a species depends on its specific ecological preferences, and the range dynamics identified for this cold-tolerant species during the last glaciation differ from species associated with warmer environments.

Multiple refugia and IBD

The use of genomic data allowed us to identify four distinct groups of populations for *P. tibetica*, which occupy the eastern, central-eastern, central and western areas of the species distribution (Figs 1, 2). These results, as well as the projected habitat at the LGM (Fig. 7c), suggest that multiple potential allopatric refugia existed for this species, probably located in the eastern, central and southwestern Himalayas. Although previous studies have

found extensive private haplotypes in populations of diverse species and suggested multiple plant refugia in the Himalayas (Opgenoorth *et al.*, 2010; Wang *et al.*, 2010b; Jia *et al.*, 2011), the clear pattern identified by our genomic-level data was not yet described in the region. For example, Opgenoorth *et al.* (2010) found that private haplotypes were evenly spread across the distribution range of a juniper complex, indicating that these junipers maintained multiple glacial (cryptic) refugia throughout their current range and underwent only localized postglacial expansions. The use of plastid and nuclear markers, which provide less resolution compared with genomic-level data, may prevent the detection of a clear pattern.

Procrustes analysis shows a high similarity score between the overall rotated genetic space and their geographic locations ($t_0 = 0.815$, $P < 10^{-5}$; Fig. 4), which is probably a result of the large-scale spatial genetic structure shaped by the refugium-driven vicariance. Long-distance dispersal and gene flow that may disturb this pattern of population structure is unlikely in *P. tibetica*, because this small herb (2–13 cm) is pollinated mainly by insects (e.g. bees) and disperses its seeds largely by gravity (Richards, 2003). Its poor ability to disperse, associated with the extreme altitudinal gradient present in the Himalayas, has probably caused fragmentation, reduced gene flow and further reinforced the genetic structure (Liu *et al.*, 2014; Wen *et al.*, 2014). IBD plays a minor role in the large-scale pattern of population structure in *P. tibetica* (Fig. 5a). However, at narrow scales, there are IBD effects on the genetic distance of populations within groups (Fig. 5). The decrease of genomic similarities between populations within groups is probably a result of limited dispersal among populations (e.g. Ferchaud *et al.*, 2010; Lanier *et al.*, 2015). However, separating the specific effects of geography and the environment on population structure is difficult (Thorpe *et al.*, 2008; Wang *et al.*, 2013). Our results show some differentiation of the ecological niches of the population (Fig. S1), but finer-scale analyses are needed to identify and quantify the importance of these variables (e.g. Lexer *et al.*, 2014).

Quaternary climatic oscillations trigger intraspecific divergence in *Primula tibetica*

The genomic data presented here provide clear evidence that intraspecific divergence in *P. tibetica* was mainly driven by Quaternary climatic oscillations. The effects of Quaternary climatic oscillations on the distribution patterns and phylogeographic structure of species in the mid- to high-latitude regions of Europe and North America (Comes & Kadereit, 1998; Abbott *et al.*, 2000; Avise, 2000; Hewitt, 2004; Anderson *et al.*, 2006; Emerson *et al.*, 2010), and in high-altitude areas (Qiu *et al.*, 2011; Liu *et al.*, 2014; Wen *et al.*, 2014; Sun *et al.*, 2015) have already been described. However, no studies yet exist for the Himalayas, and our analysis therefore provided a unique opportunity to uncover the detailed Quaternary demographic history of high-altitude populations and to better understand the processes playing a role in their distribution in this region.

The time frame of the first divergence between the eastern and central populations (groups E and C; Fig. 6) is congruent with

the largest Naynayxungla glaciation in the QTP. This event reached its maximum between 0.8 and 0.5 Ma with an ice sheet covering an area five to seven times larger than its current range (Shi, 2002; Zheng *et al.*, 2002). Such an extensive ice sheet could have caused fragmentation of ancestral populations and triggered the earliest divergence into two groups. The formation of the admixed central-eastern population (group CE) was dated to *c.* 0.37 Ma (HPD: 0.213–0.525 Ma) and coincides with the old expansion of group E (Fig. 6). During this period, the glaciation became progressively less extensive, but a cold climate is thought to have prevailed in the QTP until 0.17 Ma (Shi, 2002). The old expansion of group E may have been favored by such a cold climate, eventually resulting in a secondary contact with group C and the formation of group CE. Group W diverged from group C most likely during the LIG period when the climate was warmer (Thompson *et al.*, 1997; Shi *et al.*, 1998; Zheng *et al.*, 2002) and may have allowed the ancestral populations to colonize the western high-altitude region.

Demographic history of *Primula tibetica*

Our analyses of the demographic history of each group of populations show that all have experienced ancient expansions followed by bottlenecks (Fig. 6). The western, central and central-eastern groups of populations that occur at high altitudes have experienced only slight bottlenecks during the last glaciation (Fig. 6), a period that started from 0.07 Ma and continued until the end of the LGM in the QTP (0.01 Ma; Thompson *et al.*, 1997; Zheng *et al.*, 2002). Our ABC modeling of changes in population sizes shows that populations comprising group C experienced the most ancient expansion *c.* 1.11 Ma (HPD: 0.53–1.65 Ma), which indicates that the origin of this species probably occurred in the central Himalayas (Fig. 6). The time estimated for the most ancient expansion of this species is congruent with the divergent time from its two closely related species obtained from previous phylogenetic study (1.19 Ma, HPD: 0.51–2.13 Ma; Ren *et al.*, 2015). The current populations of group C occur at an average altitude of 4260 m (Table S1) and are thus probably adapted to live in cold environments. Their tolerance to cold might thus have facilitated the persistence of populations at high-altitude glacial refugia during past glaciations (Fig. 7c).

By contrast, the eastern populations (group E), which occur at the lowest altitude (average 2887 m; Table S1), experienced a severe bottleneck during the LIG period, but expanded during the LGM. The unusual demographic history of the eastern populations (group E) can be explained by the warmer climate in this region of the Himalayas, which displays a difference of $> 8°C$ in comparison with the region of the central populations (assuming that current temperature in the Himalayas decreases by $0.64°C$ per 100 m; Li & Zhang, 2010). The warmer interglacial period could have been detrimental for a cold-adapted species, whereas the population expansion during the LGM corresponds to a period of colder climate more similar to the situation that prevailed for its ancestral populations, but warm enough in the eastern regions to avoid extensive coverage by ice sheets (Shi *et al.*, 1998; Zheng *et al.*, 2002; Owen, 2009). Further evidence

supporting the reduction of population size during warmer periods comes from the current and MH SDMs which show restricted predicted distributions in the eastern Himalayas (Fig. 7). Nevertheless, the possible recent reduction of population size in the eastern Himalayas detected by SDM is not supported by our genomic data (Figs 6, 7). This period represents a small timescale (i.e. 18 000–25 000 yr), however, and a small density of population sampling (i.e. two populations) of group E may not provide enough information for such a recent reduction.

Finally, the western populations (group W) occur at the highest average altitude (4552 m; Table S1) and expanded during the LIG period before retreating to a southwestern refugium during the LGM (Figs 6, 7). The warm climate during the LIG period may have, in contrast to the eastern populations, facilitated expansion of this group through the opening of new potential habitats. The expansion to high-altitude areas in the western Himalayas during warmer periods is also supported by the comparison of the SDMs between the present and the MH, where more areas were predicted at present than in the MH (temperature is higher at present than the MH; Table S9). During the LGM, this area may have become too cold for this species to persist at such high altitudes as shown in the SDMs (Fig. 7). The two marginal populations that have colonized opposite geographical directions corresponding to very different altitudinal ranges are more vulnerable and respond differently to past climatic changes. Knowing the possible effect of past climatic changes on current populations may thus provide new insights into their future range dynamics in facing ongoing climatic changes and be useful for future management strategies (e.g. Lanier *et al.*, 2015).

Conclusion

We combined genomic information and SDMs to identify the processes driving the phylogeographic structure of a high-altitude plant species over a large area of the Himalayas. Our analyses demonstrate the effects of past climatic changes on the intraspecific divergence of *P. tibetica* and highlight new patterns that are important to understand the current distributions of plant species in the Himalayas. The combination of population genomics and SDMs also provides new insights to predict the impact of future climatic changes on population dynamics. Taken together, we suggest that the central Himalayas was an ancient glacial refugium throughout the Quaternary glaciations in the area. The remaining lineages have persisted in additional refugia with different responses to climatic cooling during the LGM. Our study, taken together with those recently reported for other cold-adapted species that occur in the QTP (e.g. Shimono *et al.*, 2010; Li *et al.*, 2013; Liu *et al.*, 2013), makes it clear that such species have exhibited different range dynamics (i.e. population persistence in high-altitude areas or even expansion) during the last glaciation relative to species associated with warmer environments.

Author contributions

G.R., N.S and E.C. planned and designed the research. G.R. carried out the sampling and the laboratory work, performed the molecular analysis. T.S. and N.A. participated in the initial test of the laboratory work. R.G.M. performed the SDM analysis. G.R. and N.S. wrote the manuscript with the help of R.G.M., J.L., T.S., N.A., A.G. and E.C.

References

Abbott RJ, Smith LC, Milne RI, Crawford RMM, Wolff K, Balfour J. 2000. Molecular analysis of plant migration and refugia in the Arctic. *Science* **289**: 1343–1346.

Allouche O, Tsoar A, Kadmon R. 2006. Assessing the accuracy of species distribution models: prevalence, kappa and the true skill statistic (TSS). *Journal of Applied Ecology* **43**: 1223–1232.

Anderson LL, Hu FS, Nelson DM, Petit RJ, Paige KN. 2006. Ice-age endurance: DNA evidence of a white spruce refugium in Alaska. *Proceedings of the National Academy of Sciences, USA* **103**: 12447–12450.

Avise JC. 2000. *Phylogeography: the history and formation of species.* Cambridge, MA, USA: Harvard University Press.

Catchen JM, Amores A, Hohenlohe P, Cresko W, Postlethwait JH. 2011. Stacks: building and genotyping loci *de novo* from short-read sequences. *G3: Genes Genomes, Genetics* **1**: 171–182.

Catchen J, Hohenlohe PA, Bassham S, Amores A, Cresko WA. 2013. Stacks: an analysis tool set for population genomics. *Molecular Ecology* **22**: 3124–3140.

Comes HP, Kadereit JW. 1998. The effect of Quaternary climatic changes on plant distribution and evolution. *Trends in Plant Science* **3**: 432–438.

Cornuet JM, Pudlo P, Veyssier J, Dehne-Garcia A, Gautier M, Leblois R, Marin JM, Estoup A. 2014. DIYABC v2.0: a software to make approximate Bayesian computation inferences about population history using single nucleotide polymorphism, DNA sequence and microsatellite data. *Bioinformatics* **30**: 1187–1189.

Cornuet JM, Ravigne V, Estoup A. 2010. Inference on population history and model checking using DNA sequence and microsatellite data with the software DIYABC (v1.0). *BMC Bioinformatics* **11**: 401.

Davey JW, Cezard T, Fuentes-Utrilla P, Eland C, Gharbi K, Blaxter ML. 2013. Special features of RAD sequencing data: implications for genotyping. *Molecular Ecology* **22**: 3151–3164.

Davey JW, Hohenlohe PA, Etter PD, Boone JQ, Catchen JM, Blaxter ML. 2011. Genome-wide genetic marker discovery and genotyping using next-generation sequencing. *Nature Reviews Genetics* **12**: 499–510.

Davis MB, Shaw RG. 2001. Range shifts and adaptive responses to Quaternary climate change. *Science* 292: 673–679.

Dormann CF, Elith J, Bacher S, Buchmann C, Carl G, Carre G, Marquez JRG, Gruber B, Lafourcade B, Leitao PJ *et al.* 2013. Collinearity: a review of methods to deal with it and a simulation study evaluating their performance. *Ecography* 36: 27–46.

Earl DA, vonHoldt BM. 2012. Structure Harvester: a website and program for visualizing Structure output and implementing the Evanno method. *Conservation Genetics Resources* 4: 359–361.

Emerson KJ, Merz CR, Catchen JM, Hohenlohe PA, Cresko WA, Bradshaw WE, Holzapfel CM. 2010. Resolving postglacial phylogeography using high-throughput sequencing. *Proceedings of the National Academy of Sciences, USA* 107: 16196–16200.

Evanno G, Regnaut S, Goudet J. 2005. Detecting the number of clusters of individuals using the software Structure: a simulation study. *Molecular Ecology* 14: 2611–2620.

Favre A, Päckert M, Pauls SU, Jähnig SC, Uhl D, Michalak I, Muellner-Riehl AN. 2014. The role of the uplift of the Qinghai-Tibetan plateau for the evolution of Tibetan biotas. *Biological Reviews* 90: 236–253.

Ferchaud A, Lyet A, Cheylan M, Arnal V, Baron JP, Montgelard C, Ursenbacher S. 2010. High genetic differentiation among French populations of the Orsini's viper (*Vipera ursinii ursinii*) based on mitochondrial and microsatellite data: implications for conservation management. *Journal of Heredity* 102: 67–78.

Fielding AH, Bell JF. 1997. A review of methods for the assessment of prediction errors in conservation presence/absence models. *Environmental Conservation* 24: 38–49.

Filatov DA, Osborne OG, Papadopulos AST. 2016. Demographic history of speciation in a *Senecio* altitudinal hybrid zone on Mt. Etna. *Molecular Ecology* 25: 2467–2481.

Guindon S, Dufayard JF, Lefort V, Anisimova M, Hordijk W, Gascuel O. 2010. New algorithms and methods to estimate maximum-likelihood phylogenies: assessing the PhyML 3.0. *Systematic Biology* 59: 307–321.

Guisan A, Zimmermann NE. 2000. Predictive habitat distribution models in ecology. *Ecological Modelling* 135: 147–186.

Hewitt GM. 2004. Genetic consequences of climatic oscillations in the Quaternary. *Philosophical Transactions of the Royal Society B* 359: 183–195.

Hijmans RJ, Cameron SE, Parra JL, Jones PG, Jarvis A. 2005. Very high resolution interpolated climate surfaces for global land areas. *International Journal of Climatology* 25: 1965–1978.

Hohenlohe PA, Amish SJ, Catchen JM, Allendorf FW, Luikart G. 2011. Next-generation RAD sequencing identifies thousands of SNPs for assessing hybridization between rainbow and westslope cutthroat trout. *Molecular Ecology Resources* 11: 117–122.

Holsinger KE, Weir BS. 2009. Genetics in geographically structured populations: defining, estimating and interpreting F_{ST}. *Nature Reviews Genetics* 10: 639–650.

Hoorn C, Wesselingh FP, ter Steege H, Bermudez MA, Sevink J, Sanmartin I, Sanchez-Meseguer A, Anderson CL, Figueiredo JP, Jaramillo C *et al.* 2010. Amazonia through time: Andean uplift, climate change, landscape evolution, and biodiversity. *Science* 330: 927–931.

Hu CM, Kelso S. 1996. Primulaceae. In: Wu ZY, Raven PH, eds. *Flora of China*, vol 15. Beijing, China: Science Press, St Louis, MO, USA: Missouri Botanical Garden Press, 99–185.

Hudson R. 2002. Generating samples under a Wright-Fisher neutral model of genetic variation. *Bioinformatics* 18: 337–338.

Jakobsson M, Rosenberg NA. 2007. CLUMPP: a cluster matching and permutation program for dealing with label switching and multimodality in analysis of population structure. *Bioinformatics* 23: 1801–1806.

Jia DR, Abbott RJ, Liu TL, Mao KS, Bartish IV, Liu JQ. 2012. Out of the Qinghai-Tibet Plateau: evidence for the origin and dispersal of Eurasian temperate plants from a phylogeographic study of *Hippophae rhamnoides* (Elaeagnaceae). *New Phytologist* 194: 1123–1133.

Jia DR, Liu TL, Wang LY, Zhou DW, Liu JQ. 2011. Evolutionary history of an alpine shrub *Hippophae tibetana* (Elaeagnaceae): allopatric divergence and regional expansion. *Biological Journal of the Linnean Society* 102: 37–50.

Jombart T. 2008. adegenet: a R package for the multivariate analysis of genetic markers. *Bioinformatics* 24: 1403–1405.

Lanier HC, Massatti R, He Q, Olson LE, Knowles LL. 2015. Colonization from divergent ancestors: glaciation signatures on contemporary patterns of genomic variation in Collared Pikas (*Ochotona collaris*). *Molecular Ecology* 24: 3688–3705.

Lexer C, Wüest RO, Mangili S, Heuertz M, Stölting KN, Pearman PB, Forest F, Salamin N, Zimmermann NE, Bossolini E. 2014. Genomics of the divergence continuum in an African plant biodiversity hotspot, I: drivers of population divergence in *Restio capensis* (Restionaceae). *Molecular Ecology* 23: 4373–4386.

Li L, Abbott RJ, Liu BB, Sun YS, Li LL, Zou JB, Wang X, Miehe G, Liu JQ. 2013. Pliocene intraspecific divergence and Plio-Pleistocene range expansions within *Picea likiangensis* (Lijiang spruce), a dominant forest tree of the Qinghai-Tibet Plateau. *Molecular Ecology* 22: 5237–5255.

Li JJ, Shi YF, Li BY. 1995. *Uplift of the Qinghai-Xizang (Tibet) plateau and global change*. Lanzhou, China: Lanzhou University Press.

Li WH, Zhang YG. 2010. *The vertical climate of Hengduan Mountains region and its impact on forest distribution*. Beijing, China: China Meteorological Press.

Liu JQ, Duan YW, Hao G, Ge XJ, Sun H. 2014. Evolutionary history and underlying adaptation of alpine plants on the Qinghai-Tibet Plateau. *Journal of Systematic and Evolution* 52: 241–249.

Liu J, Moller M, Provan J, Gao LM, Poudel RM, Li DZ. 2013. Geological and ecological factors drive cryptic speciation of yews in a biodiversity hotspot. *New Phytologist* 199: 1093–1108.

Liu JQ, Wang YJ, Wang AL, Hideaki O, Abbott RJ. 2006. Radiation and diversification within the *Ligularia–Cremanthodium–Parasenecio* complex (Asteraceae) triggered by uplift of the Qinghai-Tibetan Plateau. *Molecular Phylogenetics and Evolution* 38: 31–49.

Mastretta-Yanes A, Arrigo N, Alvarez N, Jorgensen TH, Piñero D, Emerson BC. 2015. Restriction site-associated DNA sequencing, genotyping error estimation and de novo assembly optimization for population genetic inference. *Molecular Ecology Resources* 15: 28–41.

Mateo RG, Felicísimo ÁM, Pottier J, Guisan A, Muñoz J. 2012. Do stacked species distribution models reflect altitudinal diversity patterns? *PLoS ONE* 7: e32586.

Mayr E. 1963. *Animal species and evolution*. Cambridge, MA, USA: Harvard University Press.

Meirmans PG, Van Tienderen PH. 2004. GENOTYPE and GENODIVE: two programs for the analysis of genetic diversity of asexual organisms. *Molecular Ecology Notes* 4: 792–794.

Meng LH, Yang R, Abbott RJ, Miehe G, Hu TH, Liu JQ. 2007. Mitochondrial and chloroplast phylogeography of *Picea crassifolia* Kom. (Pinaceae) in the Qinghai-Tibet Plateau and adjacent highlands. *Molecular Ecology* 16: 4128–4137.

Myers N, Mittermeier RA, Mittermeier CG, da Fonseca GAB, Kent J. 2000. Biodiversity hotspots for conservation priorities. *Nature* 403: 853–858.

Oksanen J, Blanchet FG, Kindt R, Legendre P, Minchin PR, O'Hara RB, Simpson GL, Solymos P, Stevens MHH, Wagner H. 2013. *vegan: Community Ecology Package*. R package v.2.0-7. URL http://CRAN.R-project.org/package=vegan.

Opgenoorth L, Vendramin GG, Mao KS, Miehe G, Miehe S, Liepelt S, Liu JQ, Ziegenhagen B. 2010. Tree endurance on the Tibetan Plateau marks the world's highest known tree line of the Last Glacial Maximum. *New Phytologist* 185: 332–342.

Owen LA. 2009. Latest Pleistocene and Holocene glacier fluctuations in the Himalaya and Tibet. *Quaternary Science Reviews* 28: 2150–2164.

Peterson BK, Weber JN, Kay EH, Fisher HS, Hoekstra HE. 2012. Double digest RADseq: an inexpensive method for de novo SNP discovery and genotyping in model and nonmodel species. *PLoS ONE* 7: e37135.

Petit RJ, Aguinagalde I, de Beaulieu JL, Bittkau C, Brewer S, Cheddadi R, Ennos R, Fineschi S, Grivet D, Lascoux M *et al.* 2003. Glacial refugia: hotspots but not melting pots of genetic diversity. *Science* 300: 1563–1565.

Pritchard JK, Stephens M, Donnelly P. 2000. Inference of population structure using multilocus genotype data. *Genetics* 155: 945–959.

Qiu YX, Fu CX, Comes HP. 2011. Plant molecular phylogeography in China and adjacent regions: tracing the genetic imprints of Quaternary climate and

environmental change in the world's most diverse temperate flora. *Molecular Phylogenetics and Evolution* 59: 225–244.

R Core Team. 2012. *R version 3.2.3: a language and environment for statistical computing*. Vienna, Austria: R Foundation for Statistical Computing.

Ren GP, Conti E, Salamin N. 2015. Phylogeny and biogeography of *Primula* sect. *Armerina*: implications for plant evolution under climate change and the uplift of the Qinghai-Tibet Plateau. *BMC Evolutionary Biology* 15: 161.

Rice WR, Hostert EE. 1993. Laboratory experiments on speciation: what have we learned in 40 years. *Evolution* 47: 1637–1653.

Richards J. 2003. *Primula*, 2nd edn. Portland, OR, USA: Timber Press.

Rosenberg NA. 2004. DISTRUCT: a program for the graphical display of population structure. *Molecular Ecology Notes* 4: 137–138.

Schorr G, Holstein N, Pearman PB, Guisan A, Kadereit JW. 2012. Integrating species distribution models (SDMs) and phylogeography for two species of Alpine *Primula*. *Ecology and Evolution* 2: 1260–1277.

Schorr G, Pearman PB, Guisan A, Kadereit JW. 2013. Combining palaeodistribution modelling and phylogeographical approaches for identifying glacial refugia in Alpine *Primula*. *Journal of Biogeography* 40: 1947–1960.

Shi YF. 2002. Characteristics of Late Quaternary monsoonal glaciation on the Tibetan Plateau and in East Asia. *Quaternary International* 97: 79–91.

Shi YF, Li JJ, Li BY. 1998. *Uplift and environmental changes of Qinghai-Tibetan Plateau in the Late Cenozoic*. Guangzhou, China: Guangdong Science and Technology Press.

Shimono A, Ueno S, Gu S, Zhao X, Tsumura Y, Tang Y. 2010. Range shifts of *Potentilla fruticosa* on the Qinghai-Tibetan Plateau during glacial and interglacial periods revealed by chloroplast DNA sequence variation. *Heredity* 104: 534–542.

Sun Y, Li L, Li L, Zou J, Liu JQ. 2015. Distributional dynamics and interspecific gene flow in *Picea likiangensis* and *P. wilsonii* triggered by climate change on the Qinghai-Tibet Plateau. *Journal of Biogeography* 42: 475–484.

Thompson LO, Yao T, Davis ME, Henderson KA, Mosley-Thompson E, Lin PN, Beer J, Synal HA, Cole-Dai J, Bolzan JF. 1997. Tropical climate instability: the last glacial cycle from a Qinghai-Tibetan ice core. *Science* 276: 1821–1825.

Thorpe RS, Surget-Groba Y, Johansson H. 2008. The relative importance of ecology and geographic isolation for speciation in anoles. *Philosophical Transactions of the Royal Society B: Biological Sciences* 363: 3071–3081.

Thuiller W, Lafourcade B, Engler R, Araújo MB. 2009. BIOMOD – a platform for ensemble forecasting of species distributions. *Ecography* 32: 369–373.

Wang LY, Abbott RJ, Zheng W, Chen P, Wang YJ, Liu JQ. 2009. History and evolution of alpine plants endemic to the Qinghai-Tibet Plateau: *Aconitum gymnandrum* (Ranunculaceae). *Molecular Ecology* 18: 709–721.

Wang IJ, Glor RE, Losos JB. 2013. Quantifying the roles of ecology and geography in spatial genetic divergence. *Ecology Letters* 16: 175–182.

Wang Q, Liu J, Allen GA, Ma Y, Yue W, Marr KL, Abbott RJ. 2016. Arctic plant origins and early formation of circumarctic distributions: a case study of the mountain sorrel, *Oxyria digyna*. *New Phytologist* 209: 343–353.

Wang H, Qiong L, Sun K, Lu F, Wang YG, Song ZP, Wu QH, Chen JK, Zhang WJ. 2010b. Phylogeographic structure of *Hippophae tibetana* (Elaeagnaceae) highlights the highest microrefugia and the rapid uplift of the Qinghai-Tibetan Plateau. *Molecular Ecology* 19: 2964–2979.

Wang C, Szpiech ZA, Degnan JH, Jakobsson M, Pemberton TJ, Hardy JA, Singleton AB, Rosenberg NA. 2010a. Comparing spatial maps of human population-genetic variation using procrustes analysis. *Statistical Applications in Genetics and Molecular Biology* 9: 13.

Wang C, Zollner S, Rosenberg NA. 2012. A quantitative comparison of the similarity between genes and geography in worldwide human populations. *PLoS Genetics* 8: e1002886.

Wen J, Zhang JQ, Nie ZL, Zhong Y, Sun H. 2014. Evolutionary diversifications of plants on the Qinghai-Tibetan Plateau. *Frontiers in Genetics* 5: 4.

Wu CY. 1987. *Flora of Tibet*. Beijing, China: Science Press.

Yan HF, Zhang CY, Wang FY, Hu CM, Ge XJ, Hao G. 2012. Population expanding with the phalanx model and lineages split by environmental heterogeneity: a case study of *Primula obconica* in subtropical China. *PLoS ONE* 7: e41315.

Yang FS, Li YF, Ding X, Wang XQ. 2008. Extensive population expansion of *Pedicularis longiflora* (Orobanchaceae) on the Qinghai-Tibetan Plateau and its correlation with the Quaternary climate change. *Molecular Ecology* 17: 5135–5145.

Yao T, Pu J, Lu A, Wang Y, Yu W. 2007. Recent glacial retreat and its impact on hydrological processes on the Tibetan Plateau, China, and surrounding regions. *Arctic, Antarctic, and Alpine Research* 39: 642–650.

Yin A, Harrison TM. 2000. Geologic evolution of the Himalayan-Tibetan orogen. *Annual Review of Earth and Planetary Sciences* 28: 211–280.

Zhang Q, Chiang TY, George M, Liu JQ, Abbott RJ. 2005. Phylogeography of the Qinghai-Tibetan Plateau endemic *Juniperus przewalskii* (Cupressaceae) inferred from chloroplast DNA sequence variation. *Molecular Ecology* 14: 3513–3524.

Zheng D. 1996. The system of physico-geographical regions of the Qinghai-Xizang (Tibet) plateau. *Science in China Series D–Earth Sciences* 39: 410–417.

Zheng BX, Xu QQ, Shen YP. 2002. The relationship between climate change and Quaternary glacial cycles on the Qinghai-Tibetan Plateau: review and speculation. *Quaternary International* 97–98: 93–101.

Zhou Z, Hong D, Niu Y, Li G, Nie Z, Wen J, Sun H. 2013. Phylogenetic and biogeographic analyses of the Sino-Himalayan endemic genus *Cyananthus* (Campanulaceae) and implications for the evolution of its sexual system. *Molecular Phylogenetics and Evolution* 68: 482–497.

Supporting Information

Additional Supporting Information may be found online in the Supporting Information tab for this article:

Fig. S1 The dispersion in environmental space of the position of 16 sampled populations used in our genomic analyses relative to the PC values for 61 *Primula tibetica* sampling locations used in the SDMs.

Fig. S2 Distribution of individuals along PC scores of genetic variation based on the analysis of SNP dataset generated by two other parameter settings ($M = 3$ and $M = 5$) in STACKS.

Fig. S3 Maximum-likelihood estimation of population relationships based on an analysis of the 2092 concatenated, unlinked SNPs; nodal support values were assessed by 1000 bootstrap replicates.

Fig. S4 Alternative demographic scenarios of *P. tibetica* analyzed by DIY-ABC and posterior probabilities of the three scenarios obtained by logistic regression of 1% of the closest simulated datasets.

Fig. S5 Alternative demographic scenarios of groups W and CW analyzed by DIY-ABC.

Fig. S6 Tests for the genetic structure based on the two thresholds of the four groups for ABC modeling of changes in population sizes.

Fig. S7 Schematic representation of ABC modeling of changes in population sizes and posterior probabilities obtained by logistic regression of 1% of the closest simulated datasets for the groups W, C, CE and E.

Fig. S8 Habitat suitability predicted by the SDMs for present, MH and LGM using four techniques.

Fig. S9 Δ*K*-values identified using Structure Harvester.

Fig. S10 Species distribution models for *Primula tibetica* at present, LIG, MH and LGM climatic conditions using three techniques.

Fig. S11 Estimates of the prior and posterior distributions of parameters revealed by the Diy-Abc modeling of the best scenario (scenario 2) for the demographic history of *Primula tibetica*.

Table S1 Locations of 16 populations of *Primula tibetica*

Table S2 Descriptions of prior settings for all parameters used in Diy-Abc

Table S3 Summary of genomic data collected for each population

Table S4 Population pairwise F_{ST} values

Table S5 Posterior probabilities of modeled scenarios obtained by logistic regression of 1% of the closest simulated datasets for ALL and groups E, CE, C and W

Table S6 Estimations of posterior distributions of parameters revealed by Diy-Abc for the best scenarios of changes in population sizes of groups E, C, CE and W, respectively

Table S7 Estimations of posterior distributions of parameters revealed by Diy-Abc for the best scenario of demographic history of *Primula tibetica*

Table S8 The differences of maximum, minimum and mean values of annual precipitation (bio12) between the current and past climatic conditions under each model for each area

Table S9 The differences of maximum, minimum and mean values of annual temperature (bio1) between the current and past climatic conditions under each model for each area

Methods S1 Species distribution models of *Primula tibetica*.

Notes S1 Abc modeling based on five genetic groups.

Please note: Wiley Blackwell are not responsible for the content or functionality of any Supporting Information supplied by the authors. Any queries (other than missing material) should be directed to the *New Phytologist* Central Office.